The Ru^{IV}=O-catalyzed sulfoxidation: a gated mechanism where O to S linkage isomerization switches between different efficiencies†

Jordi Benet-Buchholz,[a] Peter Comba,*[b] Antoni Llobet,*[a] Stephan Roeser,[a] Prabha Vadivelu[b] and Sebastian Wiesner[b]

Received 23rd November 2009, Accepted 22nd January 2010
First published as an Advance Article on the web 16th February 2010
DOI: 10.1039/b924614b

Two Ru^{IV}=O catalysts with either a pentadentate bispidine ligand L^1 or a bidentate pyrazolate L^2/terpy L^3 combination of ligands have very different efficiencies as oxygen transfer catalysts for the selective oxidation of sulfides to sulfoxides: the $[Ru^{II}(L^1)(solvent)]^{2+}$/iodosyl benzene system has an initial TOF of approx. 40 h^{-1} and quantitative yield, with $[Ru^{II}(L^2)(L^3)(solvent)]^{+}$ the initial TOF is approx. 12 h^{-1} with a maximum yield of approx. 60%. By experiment (cyclovoltametry) it is shown that there is S- to O-linkage isomerization of the Ru^{II} sulfoxide product complex, and this may partially switch off the catalytic cycle for the L^2/L^3-based catalyst. It emerges that the reasons for the reduced efficiency in the case of the L^2/L^3, in comparison with the L^1-based catalyst, are a more efficient linkage isomerization, a more stable S-bonded, in comparison with the O-bonded, Ru^{II}-based isomer, and inefficient ligand exchange in the product (hydrolysis produces the free sulfoxide and the Ru^{II} precatalyst). These interpretations are qualitatively in good agreement with preliminary DFT-based data.

Introduction

Due to the versatility of sulfoxides, the efficient and selective oxidation of sulfides is of importance in preparative organic chemistry, specifically in the area of asymmetric synthesis and enantioselective catalysis.[1-5] Ruthenium- and iron-based catalysts with pentadentate ligand systems have been found to be particularly efficient. We have used high-valent iron complexes with a variety of bispidine ligands in oxidation catalysis,[6,7] and more recently have also studied the corresponding ruthenium chemistry[8] to compare the relative reactivities and selectivities, specifically because with ruthenium there are no ambiguities with respect to the spin states.[9] Bispidines (see Chart 1 for ligand structures) are very rigid and widely variable ligand systems[10,11] and, specifically in the area of non-heme iron oxidation catalysis, have yielded a wealth of unique results.[12-14]

Here, we report the preparation and characterization of two Ru^{IV}=O-based catalysts (see Fig. 1 for the structures of $[Ru(L^1)(dmso\text{-}S)]^{2+}$ (computed structure, see below; the X-ray structures of the corresponding Cl^- and OH_2 complexes have been reported[8]) and $[Ru(L^2)(L^3)(dmso\text{-}S)]^{+}$ (X-ray crystal structure); for L^1, L^2, L^3, see Chart 1, dmso = dimethylsulfoxide), which both selectively oxidize thioanisol to the corresponding sulfoxide but with very different efficiencies. Mechanistic studies reported here indicate that the strikingly different efficiencies are due to a gated mechanism, involving for the less efficient catalyst an O to S linkage isomerization, which stabilizes the Ru^{II}-sulfoxide product and therefore prevents fast ligand exchange to allow reoxidation of Ru^{II} to the catalytically active high-valent species: if the

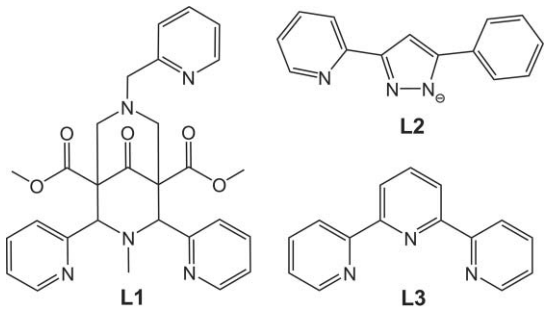

Chart 1 Structures of the three ligands used.

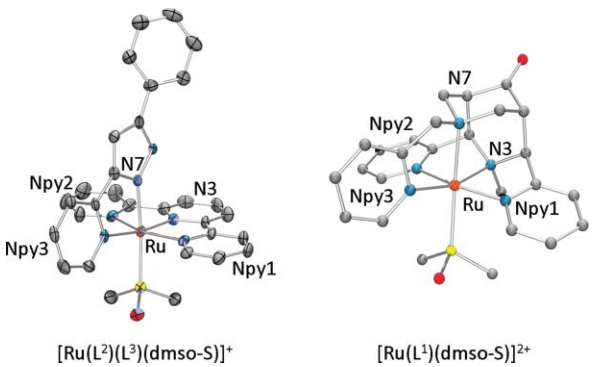

Fig. 1 Plots of the molecular structures of $[Ru(L^2)(L^3)(dmso\text{-}S)]^{+}$ (X-ray single crystal structure; ellipsoids are drawn at the 25% probability level) and $[Ru(L^1)(dmso\text{-}S)]^{2+}$ (calculated; the corresponding structure of the aqua complex has been reported[8]).

[a]*Institute of Chemical Research of Catalonia (ICIQ), Av. Països Catalans 16, E-43007 Tarragona, Spain*
[b]*Universität Heidelberg, Anorganisch-Chemisches Institut, INF 270, D-69120 Heidelberg, Germany. E-mail: peter.comba@aci.uni-heidelberg.de; Fax: +49-6221-546617*

† Electronic supplementary information (ESI) available: The electrochemical analysis of $[Ru(L^2)(L^3)(OH_2)]^{2+}$, the DFT-based computational study and crystal data. CCDC reference number 755687. For ESI and crystallographic data in CIF or other electronic format see DOI: 10.1039/b924614b

Table 1 Selected bond distances (Å) and angles (°) for $[Ru(L^1)(dmso)]^{2+}$ [a] and $[Ru(L^2)(L^3)(dmso)]^+$. Structural data of $[Ru(L^1)(OH_2)]^{2+}$ [8] appear for comparison

	$[Ru(L^2)(L^3)$-$(dmso)]^+$	$[Ru(L^1)(dmso)]^{2+}$	$[Ru(L^1)(OH_2)]^{2+}$
M–N3	1.967 (4)	2.104	2.069 (2)
M–N7	2.070 (4)	2.190	2.119 (2)
M–Npy1	2.086 (5)	2.040	2.053 (3)
M–Npy2	2.077 (5)	2.049	2.040 (3)
M–Npy3	2.128 (5)	2.086	2.040 (3)
M–X	2.265 (2)	2.267	2.134 (2)
(X = dmso, OH_2)			
Npy1–M–Npy2	159.5 (2)	163.8	163.5 (1)
N3–M–Npy3	170.7 (2)	164.1	172.2 (1)
N7–M–X	173.7 (1)	170.2	175.1 (1)
N3 ··· N7	2.953 (6)	2.92	2.91 (1)

[a] Calculated structure; geometry optimization was done using SVWN/LACVP** as implemented in the Jaguar 6.5 package.

Ru^{II}-sulfoxide product isomerizes to an inert S-bonded form, it switches off the efficient catalytic pathway. The linkage isomerization is analyzed in detail and strategies to prevent the partial inhibition and thus increase the efficiency are discussed. Preliminary data of a qualitative DFT calculation support this interpretation.

Results and discussion

The Ru^{II} complexes were obtained in good yield from equimolar amounts of $[Ru(Cl)_2(dmso)_4]$ and the ligands, refluxed for 18 h under Ar in pure MeOH.[15] The structural properties of the two complexes are rather similar to each other (see Fig. 1 and Table 1; note that the geometric parameters of the computed structure of the $[Ru(L^1)(dmso\text{-}S)]^{2+}$ complex are in good agreement with the earlier reported experimental data of the corresponding aqua complex[8]). The only possibly significant difference is that the site of the coordinated sulfoxide (dmso in the reported structures and in the electrochemical experiments, thioanisoloxide in the catalytic experiments and DFT calculations) is open in the $[Ru(L^2)(L^3)(substrate)]^+$-based system, while in the $[Ru(L^1)(substrate)]^{2+}$ system the N3-appended methyl substituent may lead to some steric congestion (see Fig. 1).

The catalytic cycle studied here (see Scheme 1) involves the usually observed oxygen transfer from the high-valent metal–oxygen fragment, Ru^{IV}=O in the present case, to the sulfur atom,

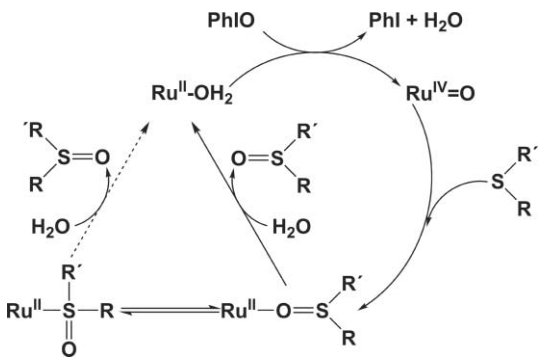

Scheme 1 Catalytic cycle for the Ru^{II}-catalyzed oxidation of sulfides to sulfoxides, involving the linkage isomerization gate Ru^{II}-O → Ru^{II}-S.

yielding a Ru^{II}-sulfoxide-O complex, which may isomerize to the corresponding Ru^{II}-sulfoxide-S intermediate;[1] by ligand exchange, both linkage isomers then produce the metal-free sulfoxide product and the Ru^{II}-OH_2 precursor complex, which, in our experiments, is reoxidized by iodosyl benzene to the active Ru^{IV}=O form. Ru^{IV}=O has been proposed before to be the active oxidant in catalytic oxidation reactions and, for other similar ligand systems, high-valent ruthenium complexes have been trapped and characterized, *e.g.* by ESI mass spectrometry.[9] Moreover, iodosyl benzene is an oxygen atom transfer agent, leading to a two electron oxidation and, in the absence of a Ru-based catalyst under otherwise identical conditions, we have shown that it is not able to oxidize sulfide substrates. The pH dependence of the one-electron potentials (Pourbaix plots) of Ru^{II} complexes has been used to show the formation of Ru^{III} and Ru^{IV} intermediates,[16,17] and the corresponding electrochemistry of $[Ru(L^1)(OH_2)]^{2+}$ has been described in detail and unambiguously demonstrates the formation of Ru^{IV}=O.[8] Similar differential pulse voltammetric measurements of the second catalyst, $[Ru(L^2)(L^3)(OH_2)]^{2+}$, at two different pH values (DPV; see ESI, Fig. S1†) show two signals for the $Ru^{III/II}$ and $Ru^{IV/III}$ redox-couples. These potentials are proton coupled one electron processes, as shown by a shift of the potential according to the Nernst equation, *i.e.* approx. 59 mV per pH unit, and therefore involve Ru^{II}-OH_2, Ru^{III}-OH and Ru^{IV}=O. A similar behavior was observed for $[Ru(L^1)(OH_2)]^{2+}$.[8]

Ligand exchange (solvation, formation of the aqua complex in the reaction studied here) of the two isomeric Ru^{II}-sulfoxide complexes (S- and O-bonded) is believed to follow a mechanism with a dissociative activation mode (I_d),[18,19] and the linkage isomer with the softer S-bonded donor is expected to be considerably more stable and, therefore, to significantly decrease the exchange rate and partially inhibit catalysis. In fact, in $[(bpy)(terpy)Ru^{II}(dmso\text{-}S)]^{2+}$ (bpy = 2,2′-bipyridine; terpy = L^3), the substitution of dmso with water has the exceedingly slow rate of k_{aq} = (1.46 ± 0.04) 10^{-5} s^{-1} at 50 °C.[20] The inertness of the two linkage isomers of the two catalysts and the corresponding exchange rates were probed experimentally by scan-rate-dependent CV of the $Ru^{III/II}$ dmso complexes (catalysis product analogs; see Fig. 2). For the $[Ru(L^1)(dmso)]^{2+}$-based system there is a much larger amount of O- than S-bonded isomer on the returning scan, when scans were at 100 mV s^{-1}. In sharp contrast, for the $[Ru(L^2)(L^3)(dmso)]^+$-based system, the amount of S-bonded isomer is much larger than the O-bonded form. The quantitative analysis of the CV's, based on a square scheme involving the linkage isomer equilibria of the oxidized and reduced forms and the two electron transfer steps[15] also shown in Fig. 2, indicates that, in the catalytically relevant Ru^{II} oxidation state (see Scheme 1), the L^1-based bispidine complex remains primarily O-bonded, while the L^2,L^3-based complex isomerizes to the more inert sulfur-bonded form (see Table 2), and this may partially block catalysis.

Indeed, the differing stability and reactivity of the O-bonded linkage isomer of the two Ru^{II} complexes leads to a remarkable difference in the catalytic efficiency (see Fig. 3). While $[Ru(L^1)(solvent)]^{2+}$, with a largely isomerization-inert Ru^{II}-dmso-O complex, is one of the most efficient Ru-based sulfoxidation pre-catalysts, $[Ru(L^2)(L^3)(solvent)]^+$ leads to a slower and less efficient catalytic transformation, and this is assumed to be due to the relatively fast isomerization to the substitution-inert S-bonded isomer. Both catalysts selectively yield the sulfoxide

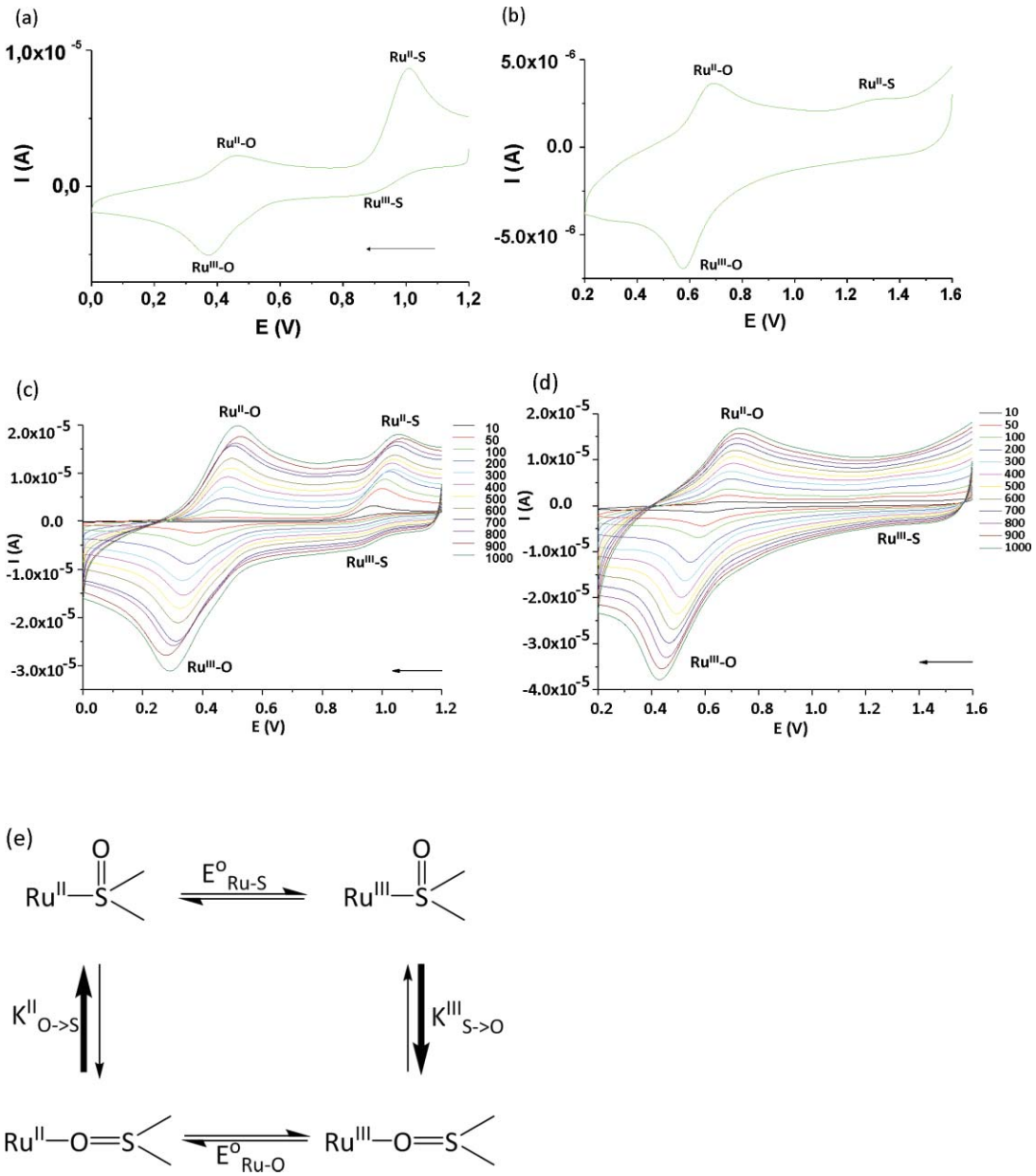

Fig. 2 Cyclic voltammograms (CV) in CH_2Cl_2 *vs.* SSCE, containing 0.1 M $TBAPF_6$, 100 mV s^{-1} of (a) 1 mM $[Ru(L^2)(L^3)(dmso)]^+$ + 4.5 mM t-BuOK; (b) 1 mM $[Ru(L^1)(dmso)]^+$; (c,d) CV's at different scan rates (in mV s^{-1}, see color code), starting at 1.2 V (c) and 1.6 V (d; before starting a scan, a constant potential of 1.2 V (a,c) and 1.6 V (b,d) for 180 s was applied to ensure complete equilibration); (e) square scheme of the electron transfer and linkage isomerization processes.

product but, under the conditions of the experiment (see Fig. 3 and Experimental), the bispidine-based catalyst has a 3 times higher initial TOF and leads to 100% conversion, while the yield with $[Ru(L^2)(L^3)(solvent)]^+$ as catalyst is only about 60% (see Fig. 3). This indicates that part of the L^2/L^3-based catalyst is inhibited and this is consistent with the hypothesis that the O- to S-isomerization of the coordinated sulfoxide is responsible for the reduced efficiency.

We have tried to support this interpretation with a density-functional-theory-based (DFT) analysis. Despite a careful validation of functionals and basis sets, the error limit, specifically with respect to the energies of the transition states and intermediates, is too large for a quantitative interpretation, and this is not unexpected and has been observed with other ruthenium-S-donor systems.[21-23] Therefore, the detailed computational results are not discussed here in detail, and these are presented, together with their interpretation, as ESI.† However, a short and qualitative analysis is warranted, specifically because this is based on relative energies and structural as well as electronic differences between analogous transition states or intermediates for very similar catalyst systems. The two main conclusions are: (i) direct ligand exchange of the Ru^{II}-sulfoxide-O product complex to complete the catalytic cycle is more efficient than linkage isomerization in both catalyst systems. This is in agreement with the observation that both Ru^{II}

Table 2 Thermodynamic and kinetic parameters for the linkage isomerization of $[Ru(L^1)(dmso\text{-}S/O)]^{2+}$ and $[Ru(L^2)(L^3)(dmso\text{-}S/O)]^{+}$, determined by scan-rate-dependent CV (see Fig. 2)

	$[Ru(L^1)(dmso)]^{2+}$	$[Ru(L^2)(L^3)(dmso)]^{+}$
$E_{1/2}$, S(V)	1.24	0.98
$E_{1/2}$, O(V)	0.68	0.41
$K^{II}_{O\rightarrow S}$	7.4×10^{7}	5.5×10^{8}
$K^{III}_{S\rightarrow O}$	6.0×10^{2}	7.81
$k^{II}_{O\rightarrow S}$ $(s^{-1})^a$	3.6×10^{-2}	2.5×10^{-1}
$k^{II}_{S\rightarrow O}$ $(s^{-1})^a$	5.0×10^{-10}	4.6×10^{-10}
$k^{III}_{O\rightarrow S}$ $(s^{-1})^a$	1.1×10^{-2}	7.7×10^{-2}
$k^{III}_{S\rightarrow O}$ $(s^{-1})^a$	6.5	6.0×10^{-1}

[a] Due to the exceedingly high stability of the O-bonded isomer, the values for $[Ru(L^1)(dmso)]^{2+}$ could only be obtained by simulation with DIGISIM.

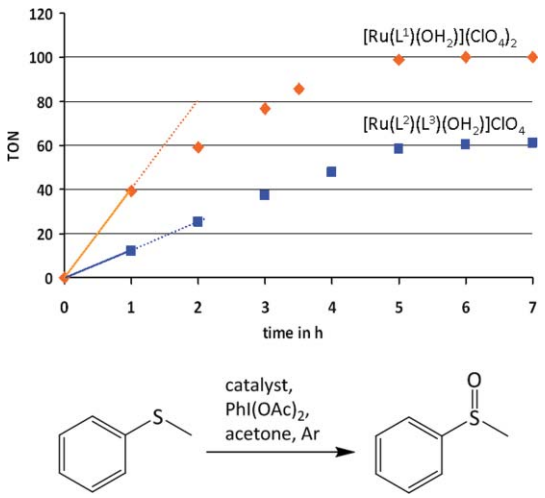

Fig. 3 Time dependence of the sulfoxidation of thioanisole, with $[Ru(L^1)(OH_2)](ClO_4)_2$ and $[Ru(L^2)(L^3)(OH_2)]ClO_4$ as catalysts and iodosylbenzene diacetate as oxidant (anaerobic conditions, in acetone; catalyst : oxidant : substrate = 1 : 100 : 1000, maximum TON of 100); initial TOF for $[Ru(L^1)(OH_2)](ClO_4)_2 = 39.5$, for $[Ru(L^2)(L^3)(OH_2)]ClO_4 = 12.1$.

complexes discussed here are catalytically active. (ii) There is a significant difference between the two systems with respect to the relative stability of the S-bonded linkage isomer: in the L^1-based system, the O-bonded isomer is the more stable, and in the L^2/L^3-based complex, it is the less stable linkage isomer. This has some consequences with respect to the corresponding energy barriers (isomerization back to the O-bonded isomer and ligand exchange from the S-bonded isomer to complete the catalytic cycle): for the more efficient L^1-based catalyst with an instable S-bonded linkage isomer, ligand exchange to reform the pre-catalyst and produce the free sulfoxide is only slightly less efficient than with the O-bonded isomer, *i.e.* the two pathways in Scheme 1 are feasible. For the L^1/L^2-based catalyst, both energy barriers for isomerization back to the O-bonded isomer and for product release are exceedingly high. That is, for the L^2/L^3-based system, there is competition between hydrolysis of the initially formed O-bonded isomer of the product complex to complete the catalytic cycle and linkage isomerization which inhibits product formation, and this is as observed experimentally, where the yield of the catalytic transformation is limited to 60%. In the L^1-based system, linkage isomerization is not a dead end, and experimentally, one therefore observes 100% transformation.

With $[Ru(L^1)(solvent)]^{2+}$, we have developed a highly efficient sulfoxidation catalyst which selectively oxidizes thioanisole to the corresponding sulfoxide in quantitative yield. The lower efficiency observed with other Ru-based catalyst systems has been analyzed by a comparison of $[Ru(L^1)(solvent)]^{2+}$ with $[Ru(L^2)(L^3)(solvent)]^{+}$. The analysis reveals that there is basically no difference with respect to the oxidation power excerted by the two catalysts but that the reduced efficiency is primarily due to a gated product release step, where linkage isomerization of the coordinated product may lead to inhibition. It is known that ligand systems with strong σ donors lead to a stabilization of the S-bonded isomer,[21,23] and it emerges that this may lead to inhibition of the catalytic activity. Subtle steric effects may be used to prevent the formation of this inactive form (destabilization of the corresponding transition state), and this is an important aspect for future developments because asymmetric ligands ideally have sterically demanding groups adjacent to the site where the Ru-O group interacts with the substrate and product.

Experimental

General

Chemicals (Aldrich, Fluka) and solvents were of the highest possible grade and used as purchased. The bispidine ligands and complexes were prepared as described before.[8,24] $[Ru(L^2)(L^3)(dmso)]^{2+}$ was prepared with a method slightly modified to that described before for similar compounds.[15] Elemental analyses were performed by the analytical laboratories of the chemical institutes of the University of Heidelberg.

Electrochemistry

Cyclic voltammetry was measured with a CH Instruments 660c potentiostat using a standard three electrode cell; a glassy carbon electrode (5 mm diameter) was used as working electrode, a Pt wire as auxiliary electrode and a SSCE electrode as reference. The samples were dissolved in degassed solvents containing the required supporting electrolyte (potassium perchlorate for water, tetrabutylammoniumperchlorate for MeOH, tetrabutylammoniumhexafluorophosphate for CH_2Cl_2; 0.1 M). Unless otherwise stated, the concentrations of the complexes were approx. 1 mM.

Catalysis

Gas chromatography was performed by capillary GC with a Varian 8000 instrument with flame ionisation detection, and equipped with a ZB-1701 column. All products from catalytic runs were identified by retention time on GC relative to authentic samples. The quantitative determination was achieved by GC, calibrated by authentic samples and with naphthalene as internal standard. General conditions for the oxidation experiments of thioanisol are given here for the reaction with $PhI(OAc)_2$ as oxidant. A known amount (approx. 68 mg (210 μmol)) of $PhI(OAc)_2$ was added at once to a solution of thioanisol (2100 μmol), the catalyst (2.1 μmol) and the internal standard naphthalene (10 mM) in acetone (4 ml) at 25 °C. Quantification of the sulfoxide product for both catalysts was done every 60 min for 7 h, using the GC setup discussed above.

X-Ray crystallography

Data collection was performed on a Bruker Nonius FR 591 system equipped with a multilayer Montel 200 mirror monochromator Mo Kα ($\lambda = 0.71073$ Å) radiation and an Apex II CCD detector. The molecular structure was solved by direct methods[25,26] and refined on F^2 by full matrix least squares techniques using the SHELX TL package with anisotropic thermal parameters.[27,28] Non-hydrogen atoms were refined anisotropically, the hydrogen atoms were placed in ideal positions.

Synthesis

[Ru(HL²)(L³)(Cl)](PF₆). A 140 mg (0.63 mmol) sample of 3-pyridyl-5-phenyl-1*H*-pyrazole (HL^2) and 305 mg (0.63 mmol) of $Ru(Cl)_2(DMSO)_4$ were dissolved in 20 ml of freshly distilled methanol, and the resulting solution was refluxed for 18 h under a static argon atmosphere. The resulting yellow solid was collected and dried in vacuum. The product was dissolved, together with 110 mg (0.473 mmol) of 2,2′:6′,2″-terpyridine, in 75 mL pure methanol and refluxed for 18 h under argon. The solvent was then removed in vacuum and the brown solid dissolved in 10 mL of a methanol/NH_4OH (aq., 28%) mixture (100 : 1). A purple solid was removed by filtration, redissolved in 60 mL of a methanol/$NH_4PF_{6(aq.,\,3\,M)}$ mixture (20 : 1) and precipitated by addition of some H_2O to the solution and then decreasing the volume to yield 167 mg of the product (0.227 mmol, 48%). Elemental analysis (%) calcd for $C_{29}H_{22}ClF_6N_6PRu{\cdot}2H_2O$: C 45.1, H 3.4, N 10.9; found: C 45.6, H 3.1, N 11.0. ^{1}H NMR (400 MHz, DMSO-d_6, see ESI for the atom numbering scheme used†): $\delta =$ 9.96 (d, $^3J_{14-13} = 5.5$ Hz, 1H; H14), 8.77 (d, $^3J_{21-22} = 8$ Hz, 2H; H21, H23), 8.67 (d, $^3J_{18-17} = 8$ Hz, 2H; H18, H26), 8.51 (d, $^3J_{11-12} =$ 8 Hz, 1H; H11), 8.32 (t, $^3J_{12-11} = {}^3J_{12-13} = 7.7$ Hz, 1H; H12), 8.18 (t, $^3J_{22-21} = 8$ Hz, 1H; H22), 7.98 (t, $^3J_{17-16} = {}^3J_{17-18} = 7.8$ Hz, 2H; H17, H27), 7.9 (t, $^3J_{1-12} = {}^3J_{13-14} = 6.6$ Hz, 1H; H13), 7.71 (s, H8), 7.64 (d, $^3J_{15-16} = {}^3J_{29-28} = 5.3$ Hz, 2H; H15, H29), 7.45 (d, $^3J_{1-2} =$ $^3J_{5-4} = 6.9$ Hz, 2H; H1, H5), 7.38 (m, 5H; H2, H3, H4, H16, H28). NOESY (400 MHz, DMSO-d_6): $\delta = 7.71$–7.45 (H8–H1 or H8–H5), 7.71–8.51 (H8–H11). $^{13}C\{^1H\}$ NMR (DMSO-d_6): $\delta = 159.7$ (C19), 159.4 (C14), 153.7 (C9), 152.5 (C15), 146.9 (C7), 137.2 (C12, C17), 134.1 (C22), 129.5 and 127.7 (C2, C3, C6, C16), 126.5 (C1), 125.1 (C13), 123.6 (C18), 122.5 (C11, C21), 122.6 (C20), 102.9 (C8). UV-vis [CH_2Cl_2; λ_{max}/nm (ε/$LM^{-1}cm^{-1}$)]: 240 (46 610), 281 (37 990), 323 (34 440), 412 (7100), 501 (8320), 655 (1448). $E_{1/2}$ Ru(II)/Ru(III): (CH_2Cl_2 + 0.1 M TBAH) 0.785 V *vs.* SSCE.

[Ru(HL²)(L³)(dmso-S)](PF₆)₂. A 200 mg (0.272 mmol) sample of $[Ru(HL^2)(L^3)(Cl)](PF_6)$ and 61.2 mg (0.272 mmol) of $AgClO_4{\cdot}H_2O$ was dissolved in 120 mL of a pre-degassed 3 : 1 mixture of acetone–H_2O. The mixture was refluxed in the absence of light and a static argon atmosphere for 4 h. After filtering the formed AgCl through a pad of Celite, 100 eq. (1.9 ml) of DMSO was added to the filtrate and the mixture was refluxed for an additional 4 h period. After precipitation of the desired complex by adding 1 mL of $NH_4PF_{6(aq.,\,3\,M)}$ and reducing the reaction volume, the orange solid was filtered off, washed with a minimum amount of H_2O and Et_2O and dried in vacuum, giving 170 mg (0.184 mmol, 68% yield) of a brown solid. Elemental analysis (%) calcd for $C_{31}H_{28}F_{12}N_6OP_2RuS{\cdot}H_2O$: C 39.5, H 3.2, N 8.9, S 3.4; found: C 39.8, H 3.2, N 8.7, S 3.2. ^{1}H NMR (400 MHz, acetone-d_6, see ESI for the atom numbering scheme used†): $\delta = 10.15$ (d, $^3J_{1-2} =$ 5.5 Hz, 1H; H1), 8.93 (d, $^3J_{21-22} = 8.4$ Hz, 2H; H21, H23), 8.78 (d, $^3J_{18-17} = 8.1$ Hz, 2H; H18, H26), 8.63 (m, 2H; H4, H22), 8.49 (t, $^3J_{3-4} = {}^3J_{3-2} = 7.4$ Hz, 1H; H3), 8.29 (t, $^3J_{17-18} = {}^3J_{17-16} = 8.0$ Hz, 2H; H17, H27), 8.18 (d, $^3J_{15-16} = 5.5$ Hz, 2H; H15, H29), 8.03 (t, $^3J_{2-3} = {}^3J_{2-1} = 6.5$ Hz, 1H; H2), 7.76 (s, 1H; H7), 7.68 (t, $^3J_{16-17} =$ $^3J_{16-18} = 6.5$ Hz, 2H; H16, H28), 7.38 (m, 5H; H10, H11, H12, H13, H14), 2.63 (s, 6H; $-CH_3$). $^{13}C\{^1H\}$ NMR (acetone-d_6): $\delta = 158.4$ (C5, C19), 158.0 (C20), 155.2 (C1), 154.3 (C15), 152.5 (C6), 149.2 (C8), 139.7 (C17), 139.0 (C3, C22), 129.1 and 126.3 (C2, C10, C11, C12, C16), 127.0 (C9), 125.3 (C18), 124.8 (C21), 123.7 (C4), 102.9 (C7), 41.7 (CH_3). UV-vis [CH_2Cl_2; λ_{max}/nm (ε/$LM^{-1}cm^{-1}$)]: 237 (34 270), 274 (44 470), 299 (28 930), 316 (25 930), 393 (6990), 475 (4015). $E_{1/2}$ Ru(II)/Ru(III): (CH_2Cl_2 + 0.1 M TBAH) 0.41 V (DMSO, O-bonded); 0.98 (DMSO, S-bonded) *vs.* SSCE.

Acknowledgements

Generous financial support by the German Science Foundation (DFG), MICINN and MEC of Spain are gratefully acknowledged for grants CSD2006-0003 and CTQ2007-67918, and for the allocation of a doctoral grant to S. R. respectively.

References

1 L. Roecker, J. C. Dobson, W. J. Vining and T. J. Meyer, *Inorg. Chem.*, 1987, **26**, 779.
2 M. H. V. Huynh, L. M. Witham, J. M. Lasker, M. Wetzler, B. Mort, D. L. Jameson, P. S. White and K. J. Takeuchi, *J. Am. Chem. Soc.*, 2003, **125**, 308.
3 O. Hamelin, S. Menage, F. Charnay, M. Chavarot, J.-L. Pierre, J. Pecaut and M. Fontecave, *Inorg. Chem.*, 2008, **47**, 6413.
4 J. Legros and C. Bolm, *Chem.–Eur. J.*, 2005, **11**, 1086.
5 A. Correa, O. Garcia Mancheno and C. Bolm, *Chem. Soc. Rev.*, 2008, **37**, 1108.
6 M. R. Bukowski, P. Comba, C. Limberg, M. Merz, L. Que Jr. and T. Wistuba, *Angew. Chem., Int. Ed.*, 2004, **43**, 1283.
7 M. R. Bukowski, P. Comba, A. Lienke, C. Limberg, C. Lopez de Laorden, R. Mas-Balleste, M. Merz and L. Que Jr., *Angew. Chem., Int. Ed.*, 2006, **45**, 3446.
8 J. Benet-Buchholz, P. Comba, A. Llobet, S. Roeser, P. Vadivelu, H. Wadepohl and S. Wiesner, *Dalton Trans.*, 2009, 5910.
9 S. N. Dhuri, M. S. Seo, Y.-M. Lee, H. Hirao, Y. Wang, W. Nam and S. Shaik, *Angew. Chem., Int. Ed.*, 2008, **47**, 3356.
10 P. Comba, M. Kerscher and W. Schiek, *Prog. Inorg. Chem.*, 2007, **55**, 613.
11 P. Comba, B. Nuber and A. Ramlow, *J. Chem. Soc., Dalton Trans.*, 1997, 347.
12 J. Bautz, M. Bukowski, M. Kerscher, A. Stubna, P. Comba, A. Lienke, E. Münck and L. Que Jr, *Angew. Chem., Int. Ed.*, 2006, **45**, 5681.
13 J. Bautz, P. Comba, C. Lopez de Laorden, M. Menzel and G. Rajaraman, *Angew. Chem., Int. Ed.*, 2007, **46**, 8067.
14 P. Comba, M. Maurer and P. Vadivelu, *J. Phys. Chem. A*, 2008, **112**, 13028.
15 C. Sens, R. M., I. Romero, A. Llobet, T. Parella, P. B. Sullivan and J. Benet-Buchholz, *Inorg. Chem.*, 2003, **42**, 2040.
16 C. Sens, M. Rodriguez, I. Romero, T. Parella, J. Benet-Buchholz and A. Llobet, *Inorg. Chem.*, 2003, **42**, 8385.
17 C. Sens, I. Romero, A. Llobet, T. Pasella and J. Benet-Buchholz, *J. Am. Chem. Soc.*, 2004, **126**, 7798.
18 N. Aebischer, E. Sidorenkova, M. Ravera, G. Laurenczy, D. Osella, J. Weber and A. E. Merbach, *Inorg. Chem.*, 1997, **36**, 6009.
19 D. De Vito, H. Siderenkova, F. P. Rotzinger, J. Weber and A. E. Merbach, *Inorg. Chem.*, 2000, **39**, 5547.
20 M. J. Root and E. Deutsch, *Inorg. Chem.*, 1985, **24**, 1464.
21 N. S. Panina and M. Calligaris, *Inorg. Chim. Acta*, 2002, **334**, 165.
22 M. Kato, T. Takayanagi, T. Fujihara and A. Nagasawa, *Inorg. Chim. Acta*, 2009, **362**, 1199.

23 M. Stener and M. Calligaris, *THEOCHEM*, 2000, **497**, 91.
24 H. Börzel, P. Comba, K. S. Hagen, M. Merz, Y. D. Lampeka, A. Lienke, G. Linti, H. Pritzkow and L. V. Tsymbal, *Inorg. Chim. Acta*, 2002, **337**, 407.
25 P. T. Beurskens, in *Crystallographic Computing 3*, ed. G. M. Sheldrick, C. Krüger and R. Goddard, Clarendon Press, Oxford, UK, 1985, p. 216.
26 P. T. Beurskens, G. Beurskens, R. de Gelder, J. M. M. Smits, S. Garcia-Granda and R. O. Gould, *DIRDIF-2008*, Radboud University Nijmegen, The Netherlands, 2008.
27 G. M. Sheldrick, *SHELXL-97, Program for refinement of crystal structures*, University of Göttingen, Germany, 1997.
28 G. M. Sheldrick, *Acta Crystallogr., Sect. A: Found. Crystallogr.*, 2008, **64**, 112.

